Enzymology:

The SUMO1-E67 Interacting Loop Peptide Is an Allosteric Inhibitor of the Dipeptidyl Peptidases 8 and 9

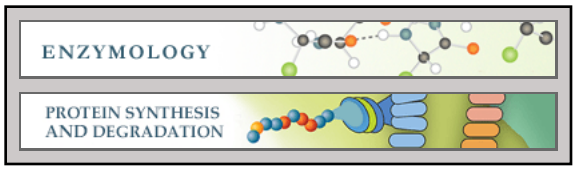

Esther Pilla, Markus Kilisch, Christof Lenz,
Henning Urlaub and Ruth Geiss-Friedlander

J. Biol. Chem. 2013, 288:32787-32796.
doi: 10.1074/jbc.M113.489179 originally published online September 26, 2013

THE JOURNAL OF BIOLOGICAL CHEMISTRY VOL. 288, NO. 45, pp. 32787–32796, November 8, 2013

The SUMO1-E67 Interacting Loop Peptide Is an Allosteric Inhibitor of the Dipeptidyl Peptidases 8 and 9*

Received for publication, May 27, 2013, and in revised form, September 25, 2013 Published, JBC Papers in Press, September 26, 2013, DOI 10.1074/jbc.M113.489179

Esther Pilla[‡], Markus Kilisch[‡], Christof Lenz[§¶], Henning Urlaub[§¶], and Ruth Geiss-Friedlander[‡1]

From the [‡]Department of Molecular Biology, Faculty of Medicine, Georg-August-University of Goettingen, 37073 Goettingen, Germany, the [§]Bioanalytical Mass Spectrometry Group, Max Planck Institute for Biophysical Chemistry, 37077 Goettingen, Germany, and the [¶]Institute for Clinical Chemistry, Faculty of Medicine, Georg-August-University of Goettingen, 37075 Goettingen, Germany

Background: SUMO1 binds to an arm motif in the prolyl-peptidase DPP9, leading to allosteric activation of the peptidase.
Results: A SUMO1 peptide covering the DPP9 interaction surface inhibits DPP9 activity. Inhibition is dependent on residues in the DPP9 arm motif.
Conclusion: The SUMO1 peptide and its variants are allosteric DPP9 inhibitors.
Significance: This work highlights the potential use of peptides mimicking interaction surfaces for modulating enzyme activity.

The intracellular peptidases dipeptidyl peptidase (DPP) 8 and DPP9 are involved in multiple cellular pathways including antigen maturation, cellular homeostasis, energy metabolism, and cell viability. Previously we showed that the small ubiquitin-like protein modifier SUMO1 interacts with an armlike structure in DPP9, leading to allosteric activation of the peptidase. Here we demonstrate that the E67-interacting loop (EIL) peptide, which corresponds to the interaction surface of SUMO1 with DPP9, acts as a noncompetitive inhibitor of DPP9. Moreover, by analyzing the sensitivity of DPP9 arm mutants to the EIL peptide, we mapped specific residues in the arm that are important for inhibition by the EIL, suggesting that the peptide acts as an allosteric inhibitor of DPP9. By modifying the EIL peptide, we constructed peptide variants with more than a 1,000-fold selectivity toward DPP8 (147 nM) and DPP9 (170 nM) over DPPIV (200 μM). Furthermore, application of these peptides to cells leads to a clear inhibition of cellular prolyl peptidase activity. Importantly, in line with previous publications, inhibition of DPP9 with these novel allosteric peptide inhibitors leads to an increase in EGF-mediated phosphorylation of Akt. This work highlights the potential use of peptides that mimic interaction surfaces for modulating enzyme activity.

Peptidases constitute 1–5% of eukaryotic genes. Remarkably, only few can cleave a peptide bond following a proline residue, because of its ridged ring structure (MEROPS Peptidase Database) (1, 2). Proteases of the S9B/dipeptidyl peptidase (DPP)[2] IV family are serine amino peptidases that have the unique ability to cleave a dipeptide bond after the amino acid proline (xP). Four active members of this family are known: DPPIV, the fibroblast activation protein α, DPP8, and DPP9 (reviewed in Refs. 1–5). Both DPPIV and fibroblast activation protein α are cell surface peptidases. Fibroblast activation protein α is expressed in embryonic tissues, is absent from adult tissue, but is expressed in tumors (6). The best characterized member of this family is DPPIV. Known DPPIV substrates include the incretin hormone glucagon-like peptide and the glucose-dependent insulinotropic polypeptide, which are important for glucose homeostasis. Consequently, DPPIV inhibitors such as sitagliptin, saxagliptin, and vildagliptin are approved drugs for treatment of type 2 diabetes (7–10). Recently, Spagnuolo *et al.* (11) showed that application of vildagliptin increases the antileukemic activity of parthenolide, suggesting that it can be used together with parthenolide for treatment of leukemia. Surprisingly, however, the authors showed that this effect was not due to inhibition of DPPIV but rather to inhibition of its intracellular homologs: DPP8 and DPP9 (11), which share ~35% homology with DPPIV.

Our understanding of the physiological roles of the two cytosolic peptidases DPP8 and DPP9 is still developing. DPP8 and DPP9 are 57% identical, with a higher conservation in their active site, corresponding to 90% amino acid identity (12–14). Not surprisingly, DPP8 and DPP9 are very similar in their catalytic properties. However, experiments with siRNA oligonucleotides show that the physiological roles of these two enzymes do not necessarily overlap; for example, DPP9, but not DPP8, is the rate-limiting enzyme for cleavage of proline-containing peptides in all tested cell lines (15).

The first identified endogenous DPP9 substrate is the tumor epitope $RU1_{34-42}$ (VPYGSFKHV). Inhibition or silencing of DPP9, but not DPP8, led to increased presentation of this antigen on MHC class I alleles to cytotoxic T-cells, linking DPP9 to the MHC class I antigen presentation pathway (Ref. 15; reviewed in Refs. 16 and 17). Recently a proteomics screen performed on DPP8 or DPP9 overexpressing cells led to the identification of 29 substrates. Among these were adenylate kinase 2 and calreticulin, suggesting a role for DPP8 and/or DPP9 in cellular homeostasis and energy metabolism (18).

* This work was supported by a Deutsche Forschungsgemeinschaft Grant 2234/1-1. SPR measurements were performed on a machine funded by Deutsche Forschungsgemeinschaft Grant 1086/2 (to M. K.).
[1] To whom correspondence should be addressed: Dept. of Molecular Biology, Georg-August-University of Goettingen, Humboldtallee 23, 37073 Goettingen, Germany. Tel.: 49-551-395984; Fax: 49-551-395960; E-mail: rgeiss@gwdg.de.
[2] The abbreviations used are: DPP, dipeptidyl peptidase; AMC, 7-amino-4-methylcoumarin; EIL, E67-interacting loop; TB, transport buffer; GP-AMC, H-Gly-Pro-7-amino-4-methylcoumarin; SPR, surface plasmon resonance.

Several lines of evidence suggest that changes in the expression level or activity of DPP8 and DPP9 are critical for cell survival and cell proliferation. Silencing of DPP8 or DPP9 in cells originating from the Ewing sarcoma family of tumors decreases cell survival and induces apoptosis (19). Inhibition of DPP8 and DPP9 with vildagliptin or the DPP8/9 inhibitor 1G244 led to reduced cell viability and apoptosis of cells from acute myeloid leukemia patients and activated macrophages (11, 20). Surprisingly, the overexpression of DPP9 also induces apoptosis (21) and attenuates EGF-mediated Akt phosphorylation in human hepatoma and human embryonic kidney cells. Of note, inhibition of Akt phosphorylation was shown to depend specifically on DPP9 but not on DPP8 activity (22).

Regulation of DPP8 and DPP9 on mRNA and protein levels was previously shown. For example, higher expression of DPP8 and DPP9 mRNA are detected in inflamed lungs (23) and chronic lymphocytic leukemia (24). Additionally, DPP9 protein levels are increased during differentiation of monocytes to macrophages; silencing of DPP9 in these cells results in reduced secretion of TNFα and IL-6 (20).

In addition to regulation of expression, DPP9 is also regulated in a post-translational manner. Recently, we showed that the small ubiquitin-like protein modifier SUMO1 acts as an allosteric activator of DPP9. By binding to an armlike motif in DPP9, SUMO1 activates peptidase activity (25). Homology structure models of DPP9 predict that this armlike structure extends from an eight-bladed propeller and is located next to a large cavity leading to the catalytic pocket in the hydrolase domain of DPP9 (26, 27). Mutations or deletions of this arm structure lead to reduced activity (25, 28), whereas SUMO1 binding to the arm leads to positive activation of DPP9 (25).

Here we asked whether it is possible to prevent allosteric activation of DPP9 by interfering with the SUMO1-DPP9 interaction. For this, we took advantage of a short peptide in SUMO1, the E67-interacting loop (EIL), which covers the association surface on the SUMO1 side and which can displace SUMO1 from preformed DPP9-SUMO1 and DPP8-SUMO1 complexes (25).

EXPERIMENTAL PROCEDURES

Cell Culture—HEK293T and HeLa cells were cultured in Dulbecco's modified Eagle's medium supplemented with 10% fetal calf serum, 1% penicillin/streptomycin, 1% L-glutamine. HEK293T cells were transfected at a confluence of 50–60% in antibiotic-free medium, according to the calcium-phosphate precipitation method.

Antibodies and Peptides—Rabbit anti-HA and rabbit anti-actin-β antibodies were obtained from Sigma. Rabbit anti-Akt and Rabbit anti-pAkt (S473) antibodies were obtained from Cell Signaling. All peptides were synthesized by Genscript (>90% purity).

Plasmids—Cloning of DPP8 and DPP9 into pFASTBacHT or pcDNA3.1 vectors (Invitrogen) was previously described (25). Single point mutations in DPP8 or DPP9 were generated using primers for site-directed mutagenesis.

Recombinant Protein Purification—DPP8 and DPP9 were generated using SF9 cells as previously described (25).

Immunoprecipitations—HEK293T cells were transfected for 48 h with HA-tagged DPP9 cloned into pcDNA3 vectors. Cells were then washed with PBS, harvested, and lysed via processing in a Dounce homogenizer in ice-cold transport buffer (TB: 20 mM Hepes/KOH, pH 7.3, 110 mM potassium acetate, 2 mM magnesium acetate, 0.5 mM EGTA, 1 mM dithiothreitol) supplemented with 0.2% Tween 20. The homogenate was centrifuged at 70,000 rpm at 4 °C for 20 min. The obtained supernatants were precleared for 30 min with protein A-coupled beads, followed by immunoprecipitation for 2 h at 4 °C with mouse anti-HA beads (Sigma). After extensive washing with TB supplemented with 0.2% Tween 20, bound proteins were eluted with 0.5 mg/ml of HA peptide in the same buffer. Immunopurified proteins were quantified via the Bradford method (Bio-Rad) and verified by Western blotting.

Kinetics Assays—All assays were performed in TB supplemented with 0.2% Tween 20. For inhibition assays, recombinant DPP9 (25 nM) purified from insect cells was incubated with 2.5 μM recombinant SUMO1 for 2 h at 4 °C before adding different concentrations of the EIL peptide. DPP9 activity was then analyzed by measuring the hydrolysis of 250 μM H-Gly-Pro-7-amino-4-methylcoumarin (GP-AMC). For peptide screenings, recombinant DPP8 or DPP9 (25 nM) were incubated with 10 μM of each peptide and immediately tested for hydrolysis of 250 μM GP-AMC. For determination of K_i, varying concentrations of inhibitory peptides were added to recombinant enzymes purified from insect cells (12.5 or 25 nM) or immunopurified from HEK293T cells (12.5 nM) prior to assaying cleavage of GP-AMC (different concentrations) in the same buffer. In all cases, fluorescence release was measured using the Appliskan microplate fluorimeter (Thermo Scientific) with 380-nm (excitation) and 480-nm (emission) filters and SkanIt software and analyzed using Prism 5.0 (GraphPad software). Each experiment was performed at least three times, in triplicate.

Peptidase Activity Assay by LC/MS/MS—For cleavage of natural DPP9 substrates, 250 μM of peptide substrate, the RU1 peptide (VPYGSFKHV) or the adenylate kinase 2 peptide (APSVPAAEPEYPKGIR) were incubated alone or in the presence of 25 nM DPP9. To test for inhibition, 10 μM peptide inhibitor (SLRFYEG) was added. All reactions were performed in TB supplemented with 0.2% Tween 20. The reactions were stopped at 0-, 15-, 45-, and 120-min time points by a 1/5,000 dilution and acidification (1/100 (v/v) in 1% formic acid, 2% acetonitrile followed by 1/50 (v:v) in 0.1% formic acid, 2% acetonitrile. The resulting samples were analyzed on a nanoLC425 nanoflow chromatography system coupled to a TripleToF 5600 Plus mass spectrometer of QqToF geometry (both AB SCIEX). In short, 5 μl of sample were preconcentrated on a self-packed reversed phase C18 precolumn (Reprosil C18-AQ; pore size, 120 Å; particle size, 5 μm; length, 4 cm; inner diameter, 0.15 cm; Dr. Maisch) and separated on a self-packed reversed phase C18 microcolumn (Reprosil C18-AQ; pore size, 120 Å; particle size, 3 μm; length, 20 cm; inner diameter, 0.075 cm) using a 10-min linear gradient (5 to 35% acetonitrile, 0.1% formic acid modifier; flow rate, 300 nl/min; column temperature, 45 °C) followed by a 5-min high organic cleaning step and a 15-min column re-equilibration. The eluent was introduced to the mass spectrom-

eter using a Nanospray 3 ion source and Desolvation Chamber Interface (AB SCIEX) via a commercial Fused Silica tip (FS360-20-10-N-C15; New Objective) at a spray voltage of 2.5 kV, a sheath gas setting of 15, and an interface heater temperature of 150 °C. The MS acquisition cycle consisted of a 500-ms TOF MS survey scan that was used for profiling of substrate and product concentrations followed by data-dependent triggering of up to five 75-ms TOF product ion spectra to confirm the identity of detected analytes. Data analysis was performed using Analyst TF 1.6 and PeakView 1.2.1 software (AB SCIEX). Analyses were performed in quadruplicate with blank injections interspersed between replicate sets.

Surface Plasmon Resonance (SPR)—Analysis was performed on a Reichert SPR Biosensor SR 7500 C instrument, using Ni^{2+} chelator chips (NiHC 1000 m) from Xantec Bioanalytics. Measurements were performed at a flow rate of 40 μl/min at 20 °C. After conditioning of the surface with 250 μl of 0.5 M EDTA, pH 8.5, and washing with immobilization buffer (10 mM Hepes, 0.15 M NaCl, 0.005% Tween 20, pH 7.4), on the surface was injected 250 μl of 0.3 M $NiSO_4$. Then His-tagged purified recombinant DPP9 (200 nM) was immobilized on the left channel, to a response value of 2500–3500 μ refractive index units. The right channel was kept empty and used as a first reference. Binding of different concentrations of EIL (25 nm to 2 μM) was measured in running buffer (10 mM Hepes, 0.15 M NaCl, 0.005% Tween 20, 50 μM EDTA, pH 7.4). Data analysis was performed using Scrubber version 2.0c. Buffer blanks were used as a second reference.

Peptidase Activity from Cell Extracts—For EIL peptide inhibition in lysates, HeLa cells were washed in PBS, harvested, processed in a Dounce homogenizer in ice-cold TB, and then centrifuged at 70,000 rpm at 4 °C for 20 min. 6-μg cytosolic extracts were then incubated with 27 μM of either SUMO1-EIL peptide (SLRFLFEGQRIADNH) or SUMO1-control peptide (SSEIHFKVKMTTHLK). Lysates were immediately analyzed for hydrolysis GP-AMC, Lys-Pro-AMC (KP-AMC), Ala-Ala-Phe-AMC (AAF-AMC), and Arg-AMC (R-AMC).

Transduction of Inhibitory Peptides into Cells—Inhibitory peptides were allowed to form a complex with the cell-penetrating peptide (Peptide-1) in DMEM FCS-free at molar ratios of 1:10 or 1:20 (cargo:carrier). Complexes were formed for 30 min at 37 °C. The mixtures were then overlaid onto HeLa cells 60–70% confluent, allowing the complexes to enter the cells for 30 min at 37 °C. For analysis of activity, peptide-transduced HeLa cells were lysed in ice-cold TB supplemented with 0.2% Tween. After ultracentrifugation, 4 μg of lysates were tested for prolyl-peptidase activity using 250 μM GP-AMC. Each experiment was performed in triplicate. For testing of EGF-mediated Akt phosphorylation, HeLa cells were overlaid with the pep1-SLRFLYAG or SLRFLYEG complexes for 25 min at 37 °C, followed by a 5-min stimulation with 10 ng/ml EGF. Cells were washed with PBS and directly lysed in sample buffer for analysis on SDS-PAGE followed by Western blotting.

RESULTS

The SUMO1 EIL Peptide Inhibits Prolyl Peptidase Activity in Cell Lysates—Previously we showed that the SUMO1-EIL peptide (SLRFLFEGQRIADNH) can dissociate a DPP9-SUMO1 complex (25). Here we asked whether the EIL can prevent SUMO1-mediated activation of DPP9, by competing out the interaction of SUMO1 with DPP9. As shown in Fig. 1, incubation of cell lysates with the EIL peptide leads to a clear reduction in the capacity of these lysates to hydrolyze artificial DPP substrates such as GP-AMC and KP-AMC (Fig. 1, *A* and *B*). This effect was specific for the EIL and not observed in the presence of a control peptide also originating from SUMO (SSEIHFKVKMTTHLK) but not participating in the DPP9-SUMO1 interaction (25). Importantly, the EIL did not inhibit the hydrolysis of R-AMC or AAF-AMC, which are not substrates for DPP enzymes (Fig. 1, *C* and *D*). Taken together, these results show for the first time that the EIL specifically inhibits prolyl peptidase activity in cell lysates.

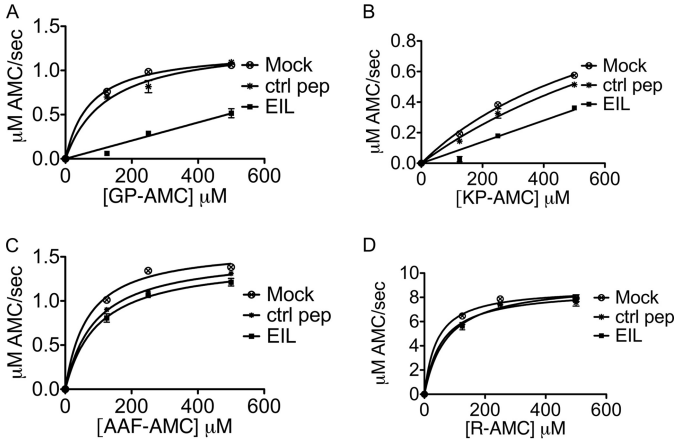

FIGURE 1. **The EIL peptide inhibits prolyl peptidase activity in cell lysates.** *A–D*, cytosolic extracts from HeLa cells were incubated with 27 μM SUMO1-EIL peptide (SLRFLFEGQRIADNH) or SUMO1-control peptide (SSEIHFKVKMTTHLK). Lysates were immediately analyzed for hydrolysis of GP-AMC (*A*), KP-AMC (*B*), AAF-AMC (*C*), and R-AMC (*D*). All experiments described were performed at least three times, in triplicate. *ctrl*, control.

The SUMO1 EIL Peptide Is a Novel Noncompetitive Inhibitor of DPP8 and DPP9—To further study the inhibitory mechanism of the EIL-peptide, we tested its effect on purified recombinant DPP9 in complex with SUMO1. In line with our previous results, DPP9 was activated by 2.5 μM SUMO1, as measured by a 25% increase in GP-AMC hydrolysis (Fig. 2*A*) (25). To reverse this effect, the activity of the SUMO1-DPP9 complex was measured in the presence of 27 or 55 μM EIL peptide. Under these conditions, we could not observe activation of DPP9 by SUMO1 (Fig. 2*A*). Surprisingly, in the presence of the EIL peptide, DPP9 activity was lower compared with the activity of DPP9 alone (Fig. 2*A*, *Mock*), suggesting that the inhibitory effect of the EIL peptide is higher than expected solely because of the dissociation of the SUMO1-DPP9 complex (Fig. 2*A*). Moreover, as shown in Fig. 2*B*, the EIL inhibits recombinant DPP9, also in the absence of SUMO1 (Fig. 2*B*). We tested for direct binding between the EIL and DPP9 using SPR experiments. Using this setup, we verified direct association of the EIL with DPP9, with a K_D value of 396.011 nM (Fig. 2, *C* and *D*).

The inhibition kinetics of DPP9 by the EIL indicates that in contrast to all other published DPP inhibitors, the EIL acts as a noncompetitive inhibitor (Fig. 2*B*). Because the EIL is a SUMO1 peptide, we asked whether its inhibitory effect is dependent on Val-285 in the DPP9 arm motif, which is essential

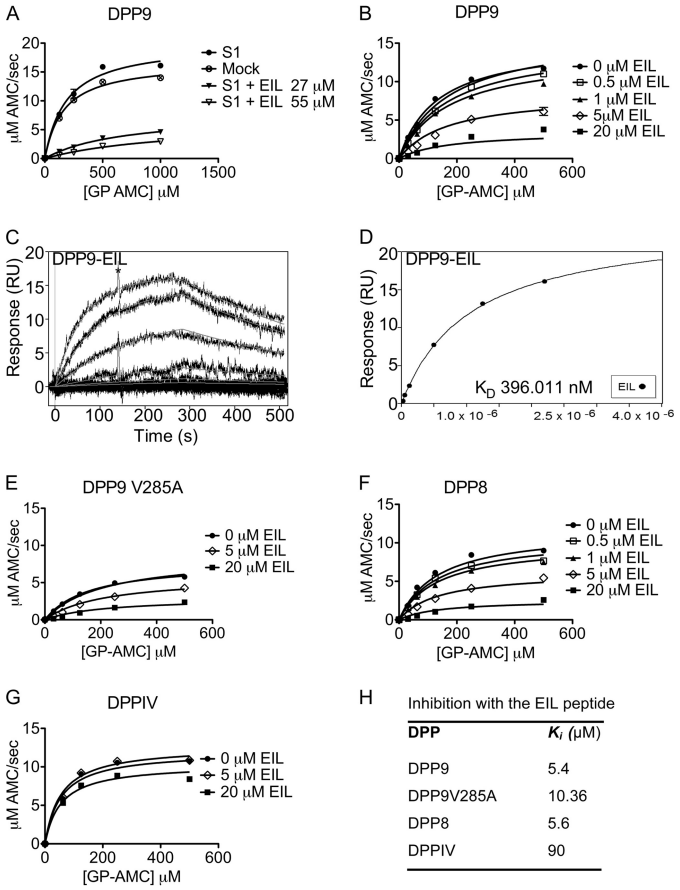

H

Inhibition with the EIL peptide

DPP	K_i (μM)
DPP9	5.4
DPP9V285A	10.36
DPP8	5.6
DPPIV	90

FIGURE 2. **The EIL peptide is a noncompetitive inhibitor of DPP8 and DPP9.** *A–H*, His-tagged recombinant enzymes purified from insect cells. All experiments described were performed at least three times, in triplicate. *A*, DPP9 (25 nM) was incubated with SUMO1 (2.5 μM). Following complex formation, the EIL peptide was added (27 or 55 μM), and DPP9 was tested for the hydrolysis of GP-AMC. *B*, shown is a Michaelis-Menten analysis for 25 nM DPP9. K_i values were calculated in the absence or presence of varying concentrations of the EIL peptide, assuming noncompetitive inhibition. Mock samples are used for control and contain DPP9 alone. *C*, DPP9 was immobilized on a Ni^{2+} chelator chip surface. SPR response was recorded after injecting 25, 50, 100, 500, 1,000, and 2,000 nM EIL. A typical sensogram is shown. *Black lines* show observed binding, and *thin solid lines* show global fit of obtained data using kinetic parameters k_a and k_d. The outstanding peak marked by an *asterisk* corresponds to a pump refill during the measurement. *D*, equilibrium binding analysis of DPP9 and EIL at 20 °C. The equilibrium binding constant (K_D) was obtained using a nonlinear curve fit. *E*, activity of the DPP9 SUMO-binding arm mutant V285A was measured as in *B*. *F*, activity of DPP8 was measured as in *B*. *G*, activity of DPPIV was measured as in *B*. *H*, table summarizing the K_i values for inhibition by the EIL peptide.

for its interaction with SUMO1 (15). In line with the importance of Val-285 for interaction with SUMO1, the DPP9 V285A mutant is also less sensitive to the EIL peptide, as measured by an increased K_i value of 10.36 μM compared with 5.4 μM for the wild-type enzyme (Fig. 2*E*). In line with our previous findings showing that both DPP8 and DPP9 interact with SUMO1, here we find that DPP8 is also inhibited by the EIL, to a similar extent as DPP9, with a K_i value of 5.6 μM (Fig. 2*F*). On the other hand, DPPIV is significantly less sensitive to the EIL, with a K_i value of 90 μM (Fig. 2, *G* and *H*). Taken together, these results show that the EIL peptide, originating from SUMO1, is a novel, noncompetitive inhibitor of DPP9, which relies on Val-285 in the arm motif. The inhibitor shows selectivity for DPP8 and DPP9 over DPPIV.

TABLE 1

Mapping of residues in the DPP9 arm that affect the enzymatic activity or the sensitivity to the EIL

Activity of HA-tagged wild-type and arm mutant DPP9 variants purified from HEK293T cells. K_{cat} (s^{-1}) and K_m values (μM) of DPP9 (12.5 nM) wild-type and arm mutants. K_i values (μM) were calculated in the absence or presence of varying concentrations of the EIL peptide, assuming noncompetitive inhibition. Marked in bold are mutants that are only slightly impaired in enzymatic activity but show reduced sensitivity to the EIL peptide. ND, not determined.

Protein	K_{cat}	K_m	K_{cat}/K_m	K_i (EIL)
DPP9	587.2	55.5	10.6	4.2
DPP9 Y277A	126.4	40.7	3.1	4.4
DPP9 E278A/E279A	Inactive	Inactive	Inactive	ND
DPP9 D281A/E282A	Inactive	Inactive	Inactive	ND
DPP9 V285A	310.4	158.9	1.9	10.4
DPP9 E286A	371.1	60.4	6.2	4.5
DPP9 I288A	346.1	40.4	8.6	4.1
DPP9 H289A	270.9	50.9	5.3	3.9
DPP9 V290A	324.7	39.5	8.2	4.0
DPP9 S292A	146.6	47.3	3.1	4.5
DPP9 L295A	**712.4**	**80.1**	**8.9**	**6.5**
DPP9 E296A/E297A	718.4	66.1	10.9	4.5
DPP9 R298A	434.8	98.8	4.4	6.3
DPP9 K299A	273.4	55.9	4.9	4.8
DPP9 D301A	414.8	244.2	1.7	13.9
DPP9 Y303D	**610.4**	**68.9**	**8.9**	**9.3**
DPP9 Y305D	87.9	865.2	0.1	40.0
DPP9 Y305A	243.4	798.9	0.3	45.5

Mapping of Residues in the Arm Important for DPP9 Sensitivity to the EIL: Leu-295 and Tyr-303—DPP9 V285A mutant shows reduced sensitivity to the EIL peptide but is also impaired in catalytic activity. The K_{cat} value of V285A mutant is 310 s^{-1} compared with the wild-type enzyme with a K_{cat} value of 608 s^{-1} (Fig. 2, *B* and *E*). We asked whether there are residues that when mutated they are less sensitive to the EIL without impairing DPP9 enzyme activity. For this, we constructed several DPP9 arm mutants, which we expressed and purified from HEK293T cells. All mutants were first tested for enzymatic activity. Of note, wild-type DPP9 purified from HEK293T cells showed a slightly reduced K_i (4.2 μM) compared with a recombinant DPP9 expressed and purified from insect cells (5.4 μM). Therefore, all mutants purified from HEK293T cells were compared in their sensitivity to the wild-type protein, purified in the same way, also from HEK293T cells. As shown in Table 1, most of the DPP9 arm mutants were less active compared with the wild-type enzyme, however, to a different extent. Strongest reduction in activity was measured for DPP9 variants mutated at Glu-278–Glu-279, Asp-281–Glu-282, or Tyr-305, emphasizing the importance of these specific residues in the arm for DPP9 activity.

Although mutations of the arm can lead to clear changes in enzymatic parameters, most mutants displayed a similar sensitivity to the EIL peptide, as the wild-type protein expressed in HEK293T cells (K_i 4.19 μM). This was seen for example for DPP9 S292A or Y277A mutants with a clearly reduced K_{cat} value and the DPP9 E296AE297A mutant with an increased K_m value (Table 1 and Fig. 3, *top left* and *right panels*).

However, some DPP9 variants mutated in Leu-295, Arg-298, Asp-301, Tyr-303, or Tyr-305 showed a clear reduction in sensitivity to the EIL peptide, as measured by an increase in the K_i values compared with the wild-type protein. Notably, although DPP9 mutated at Leu-295 (K_i = 6.5 μM) or Tyr-303 (K_i = 9.2 μM) was less sensitive to the EIL compared with the wild-type enzyme (K_i = 4.2 μM), these mutants were only slightly

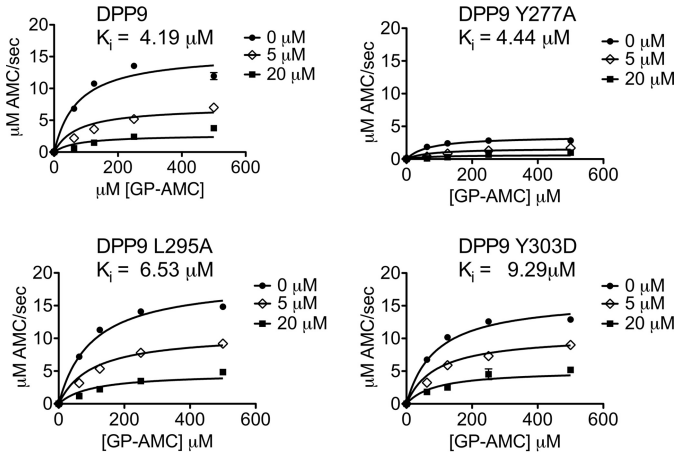

FIGURE 3. **Leu-295 and Tyr-303 in the DPP9 arm are important for sensitivity to the EIL.** Inhibition of HA-tagged wild-type and arm mutant DPP9, by the EIL. Shown are Michaelis-Menten analyses for 12.5 nM HA-tagged DPP9 variants purified from HEK293T cells. Each experiment was performed at least three times, in triplicate. *Top left panel*, wild-type DPP9. *Bottom left* and *right panels*, DPP9 Y277A. *Bottom left panel*, DPP9 L295A. *Bottom right panel*, DPP9 Y303D.

impaired in their catalytic activity (Table 1 and Fig. 3, *bottom left* and *right panels*). These results demonstrate the importance of selective residues in the DPP9 arm for sensitivity to the EIL peptide, with only a minor effect on general enzyme kinetics.

Improved DPP8 and DPP9 Inhibition by Truncated EIL Variant Peptides—To increase the inhibitory effect on DPP8 and DPP9, we designed a peptide library containing truncated versions of the EIL peptide (Table 2 and data not shown). In this screen, recombinant DPP8 and DPP9 were tested for the hydrolysis of GP-AMC in the presence or absence of the peptide variant. Shortening of the EIL peptide from the amino terminus by removal of the first serine strongly reduced the inhibitory effect of the peptide variant toward both DPP8 and DPP9, showing more than 80% residual activity compared with control reactions in the absence of an inhibitory peptide. On the other hand, peptide variants shortened from the carboxyl terminus were more effective inhibitors compared with the EIL. A peptide with the minimal sequence SLRFLFEG was most effective in inhibition of both DPP8 (K_i of 4 μM) and DPP9 (K_i = 1.3 μM) compared with the EIL peptide (K_i 5.4 μM) (Table 2 and Fig. 4*A*).

In a subsequent step, we modified the SLRFLFEG peptide to increase the efficiency of inhibition (Fig. 4*A*). Interestingly, two peptide variants, SLRFL**W**EG and SLRFL**YA**G, displayed a 4–4.5-fold higher selectivity toward DPP8 over DPP9. Of all tested peptides, the most efficient inhibitor was SLRFL**Y**EG, with K_i values of 0.147 and 0.17 μM for DPP8 and DPP9, respectively, more than 30-fold lower compared with the inhibition of DPP8 and DPP9 with EIL peptide (Fig. 4, *B* and *C*). Surprisingly, replacing Phe in position 4 by a Tyr, strongly impaired the inhibitory effect of SLR**Y**L**Y**EG (Fig. 4*A*), showing more than 130- and 170-fold decreases in inhibition of DPP8 and DPP9, respectively, compared with the SLRFLYEG.

Importantly, SLRFLWEG and SLRFLYEG show a significant increase not only in efficiency but also in selectivity toward DPP8 and DPP9, compared with DPPIV. Whereas the K_i values for DPP8 and DPP9 are in the nanomolar range, DPPIV is

TABLE 2

The amino-terminal part of the EIL peptide is the minimal sequence for DPP8 and DPP9 inhibition

Truncated versions of the EIL peptide (10 μM) were tested for inhibition of recombinant DPP8 and DPP9 expressed and purified from insect cells. The percentage of residual activity was calculated in comparison to enzymatic activity in the absence of inhibitory peptide. Marked in bold is the minimal sequence that gives the strongest inhibition.

Peptide sequence	Residual activity	
	DPP8	DPP9
	%	%
SLRFLFEGQRIADNH	55.74	45.51
LRFLFEGQRIADN	78.32	82.9
RFLFEGQRIAD	43.56	57.27
FLFEGQRIA	76.49	83.94
FLFEGQRI	80.8	91.03
LFEGQR	76.98	86.17
FLIEGQRI	72.92	83.28
LRFLFEGQRIADNH	81.47	95.4
RFLFEGQRIADNH	60.37	50.32
LFEGQRIADNH	77.89	88.55
FEGQRIADNH	90.16	93.04
SLRFLFEGQRIAD	40.3	43.13
SLRFLFEGQRI	40.2	35.96
SLRFLFEGQR	30.97	30.55
SLRFLFEGQ	23.87	26.13
SLRFLFEG	**17.69**	**18.05**

inhibited by both peptides with a K_i higher than 200 μM (Fig. 4, *B–D*). Therefore, the selectivity toward DPP8 and DPP9 by both peptides is more than a 1000-fold compared with DPPIV. For comparison, the EIL peptide showed only a 16-fold selectivity toward DPP8 and DPP9.

SLRFLYEG Inhibits the Processing of Natural DPP9 Substrates—Because DPP9 kinetics described so far were performed on the artificial GP-AMC substrate, next we tested whether SLRFLYEG also affects the cleavage of natural DPP9 substrates. For this, we analyzed the processing of $RU1_{34-42}$, an antigen peptide (VPYGSFKHV), which we previously showed to be an endogenous DPP9 substrate (15). As shown in Fig. 5, mass spectrometry analysis demonstrates that DPP9 removes two residues (VP) from the $RU1_{34-42}$ peptide in a time-dependent manner. Importantly, processing of the $RU1_{34-42}$ peptide by DPP9 is clearly inhibited in the presence of SLRFLYEG, compared with control samples containing DPP9 and $RU1_{34-42}$ alone (Fig. 5*A*). In addition, we also assayed the cleavage of an amino-terminal peptide originating from adenylate kinase 2 (APSVPAAEPEYPKGIR), which was recently identified in a proteomics screen for DPP9 substrates and shown to be processed *in vitro* by recombinant DPP9 (18). As shown in Fig. 5*B*, the processing of the adenylate kinase 2 by DPP9 is also clearly inhibited by the SLRFYEG peptide (Fig. 5*B*). Taken together, these results show that the SLRFYEG peptide is a novel DPP9 inhibitor, affecting the processing of not only artificial substrates but also of natural DPP9 substrates.

Inhibition of Endogenous DPP8 and DPP9 Activity by the SLRFLYEG and Its Variants—Having shown that SLRFLYEG and its variants are novel allosteric DPP8 and DPP9 inhibitors, we next asked whether these could be applied as a tool for inhibition of DPP8 and DPP9 activity in intact cells.

To deliver these peptide inhibitors into cells, we took advantage of Pep-1, (KETWWETWWTEWSQPKKKRKV), a well characterized carrier peptide. Pep-1 is known to improve the translocation of its cargo, through the plasma membrane, leav-

A

Peptide	K_i (nM) for DPP8	K_i (nM) for DPP9
SLRFLFEG	4068 ± 349.7	1337 ± 90.52
SLRFLWEG	256.4 ± 16.15	1121 ± 66.15
SLRFLYDG	167.2 ± 11.13	179 ± 15.79
SLRFLYEG	**147 ± 11.13**	**170 ± 11.28**
SLRFLYAG	200 ± 20.70	739.8 ± 53.2
SLRYLYEG	23120 ± 1180	35210 ± 2085

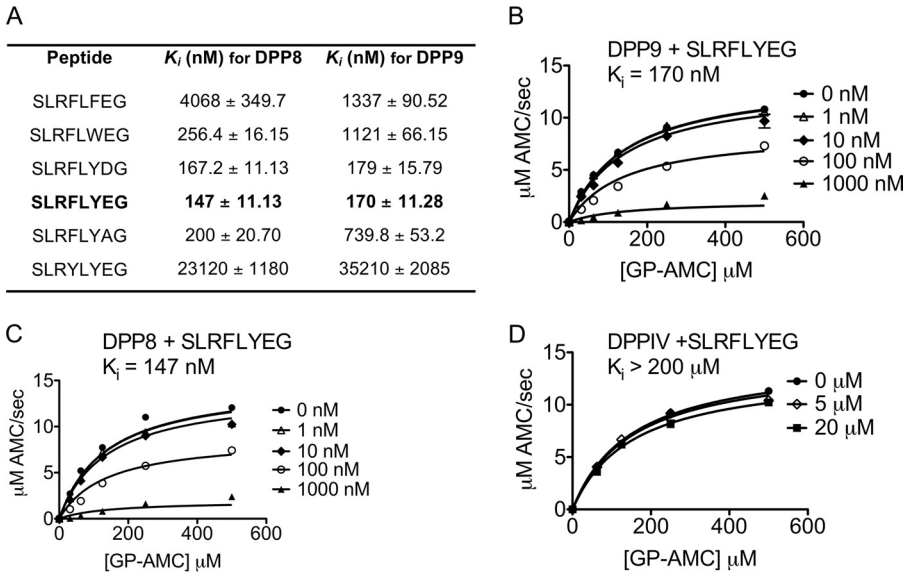

FIGURE 4. **SLRFLYEG, a highly selective and efficient DPP8 and DPP9 inhibitor.** *A*, table summarizing the K_i values for inhibition of recombinant DPP8 and DPP9 (purified from insect cells) by peptide variants, calculated in the presence of varying concentrations of the tested peptides, assuming noncompetitive inhibition. *B–D*, kinetic curves for inhibition of DPP9 (*B*), DPP8 (*C*), and DPPIV (*D*) in the presence of the indicated SLRFLYEG concentrations. All experiments described were performed at least three times, in triplicate.

ing the biochemical properties of the cargo unchanged (Ref. 29; reviewed in Refs. 30 and 31). This method allows us to deliver the SLRFLYLEG peptide variants to a comparable efficiency and compensate for the differences in the Grand average hydrophobicity. To test for inhibition of DPP8 and DPP9 activity in the cytosol, cells were treated for 30 min with SLR*X*L*XX*G inhibitory peptides complexed with Pep-1. The cells were then lysed, and the capacity of the cytosolic extracts to cleave the model substrate GP-AMC was analyzed. Using this setup, we detect a 30% drop in the cytosolic prolyl peptidase activity in cells exposed to 5 μM SLRFLYEG compared with the control cells treated with Pep-1 alone (Fig. 6*A*). A similar decrease in cytosolic prolyl-peptidase activity was also achieved for cells incubated with 5 μM SLRFLYAG and SLRFLWEG (Fig. 6, *B* and *C*). For control, we treated cells with SLRYLYEG, which is less efficient in inhibition of DPP8 and DPP9 as measured by higher K_i values compared with SLRFLYEG (Fig. 4*A*). To compensate for the lower inhibition efficiency, we treated cells with 10 μM inhibitor peptide instead of 5 μM. Under these conditions, exposure of cells to SLRYLYEG caused a 20% drop in cytosolic prolyl peptidase activity compared with control cells (Fig. 6*D*). Taken together, these results validate the inhibition of endogenous DPP8 and DPP9 by SLRFLYEG, SLRFLYAG, and SLRFLWEG. Because inhibition of cytosolic prolyl peptidase activity was observed already by treating cells with 5 μM SLRFLYEG, it is highly unlikely that the inhibition results from unspecific inhibition of the extracellular peptidase DPPIV, which shows a $K_i > 200$ μM for this peptide (Fig. 4*D*).

To obtain further proof for the inhibition of endogenous DPP9 by SLRFLYEG and SLRFLYAG within cells, we tested the effect of these inhibitors on EGF-mediated Akt phosphorylation. Previously, it was shown that DPP9, but not DPP8 overexpression, leads to attenuation of EGF-mediated Akt phosphorylation and that treatment of cells overexpressing DPP9 with a competitive DPP8/9 inhibitor lead to increased Akt phosphorylation upon EGF treatment (22). To analyze whether inhibition of DPP9 by SLRFLYEG and SLRFLYAG would have a similar effect to the inhibition of these peptidases by a competitive DPP8/9 inhibitors, HeLa cells were treated for 25 min with the peptide inhibitors, followed by a 5 min stimulation with EGF (Fig. 6, *E* and *F*). Analysis of these EGF-treated samples showed that indeed treatment of HeLa cells with these novel inhibitors SLRFLYEG and SLRFLYAG leads to an increase in EGF-mediated phosphorylation of Akt, compared with untreated cells (Fig. 6, *E* and *F*). Of note, in our setup, cells were not overexpressing DPP9, showing that inhibition of endogenous DPP9 with these novel noncompetitive allosteric inhibitors is sufficient for modulating the Akt pathway. Taken together, these results demonstrate the applicability of SLRFLYEG and SLRFLYAG for studying the roles of endogenous DPP9 and DPP8 in cells.

DISCUSSION

Previously we showed that the arm of DPP9 is an important site for allosteric regulation of the peptidase and identified SUMO1 as the first allosteric activator of DPP9 (25). As a continuation of this work, here we show that the SUMO1-EIL peptide, which covers the interaction surface of SUMO1 with DPP9, inhibits both DPP9 and DPP8, with K_i values in the low micromolar range. Furthermore, by designing and modifying shorter variants of the EIL peptide, we increased the efficiency of inhibition. The most effective inhibitor we obtained was SLRFLYEG, with K_i values of 147 nM for DPP8 and 170 nM for DPP9, a more than 35-fold increase in efficiency compared with the EIL. Importantly, we verified that treating DPP9 with SLRFLYEG inhibits not only the degradation of artificial (GP-AMC) substrates but also the degradation of a peptide originating from adenylate kinase 3, which was recently identified as a DPP9 substrate candidate in a large proteomics screen, and the

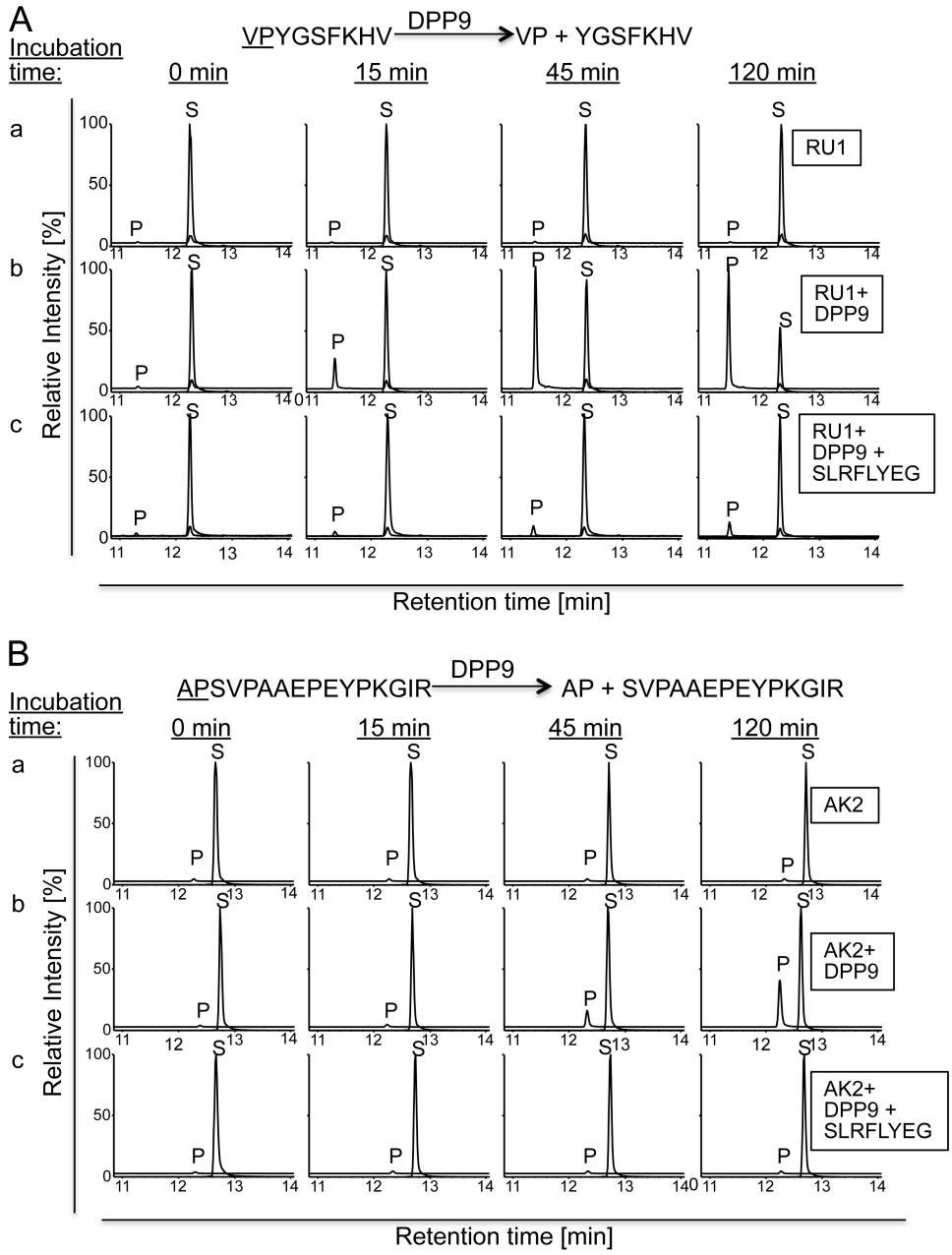

FIGURE 5. **SLRFLYEG inhibits the cleavage of native DPP9 substrates, assayed by nanoLC/MS/MS.** *A*, synthetic RU1 peptide (VPYGSFKHV) was incubated either alone (*row a*), with 25 nM DPP9 (*row b*), or with 25 nM DPP9 and 10 μM EIL peptide inhibitor SLRFYEG (*row c*). Aliquots were taken at 0-, 15-, 45-, and 120-min time points, the enzymatic reactions were stopped by dilution/acidification, and the resulting samples were analyzed by high resolution liquid chromatography/tandem mass spectrometry. All mass spectrometry analysis were performed in quadruplicate. Representative experiments per time point are shown. The panels show extracted ion chromatograms for both substrate VPYGSFKHV (labeled *S*, $[M+2H]^{2+}$ *m/z* 517.2769; retention time, 12.3 min) and product YGSFKHV (labeled *P*, $[M+2H]^{2+}$ *m/z* 419.2163; retention time, 11.4 min; trace offset by 4%). The identity of the product peak was established both by accurate mass measurement within 5 ppm and by product ion spectra (data not shown). Small peaks were observed at all time points for product P and attributed to a peptide synthesis side product (11.4 min) and in-source fragmentation of the substrate (12.3 min). *Row b* clearly demonstrates the dipeptidylpeptidase activity of DPP9 on the substrate, whereas *row c* shows inhibition by the EIL peptide. *B*, synthetic adenylate kinase 2 (*AK2*) peptide (APSVPAAEPEYPKGIR) was incubated either alone (*row a*), with 25 nM DPP9 (*row b*), or with 25 nM DPP9 and 10 μM EIL peptide inhibitor SLRFYEG (*row c*). Aliquots were taken and analyzed as described for *A*. The panels show extracted ion chromatograms for both substrate APSVPAAEPEYPKGIR (labeled *S*, $[M+3H]^{3+}$ *m/z* 561.3018; retention time, 12.7 min) and product SVPAAEPEYPKGIR (labeled *P*, $[M+3H]^{3+}$ *m/z* 505.2718; retention time, 12.3 min; trace offset by 4%). The identity of the product peak was established both by accurate mass measurement within 5 ppm and by product ion spectra (data not shown). Small peaks were observed at all time points for product P and attributed to peptide synthesis side products (12.3 min). *Row b* clearly demonstrates the dipeptidylpeptidase activity of DPP9 on the substrate, whereas *row c* shows inhibition by the EIL peptide.

degradation of the endogenous DPP9 substrate, the $RU1_{34-42}$ antigenic peptide.

Enzyme kinetics shows that the EIL and its variants act as noncompetitive inhibitors. Furthermore, we mapped residues in the DPP9 arm, which are important for sensitivity of the enzyme to the EIL and SLRFLYEG. In our analysis of the DPP9-SUMO1 interaction, we previously identified residues in the arm motif of DPP9 as being important for interaction with SUMO1, most prominently Val-285. In line with this, the DPP9V285A is also less sensitive to the inhibitory effect of the

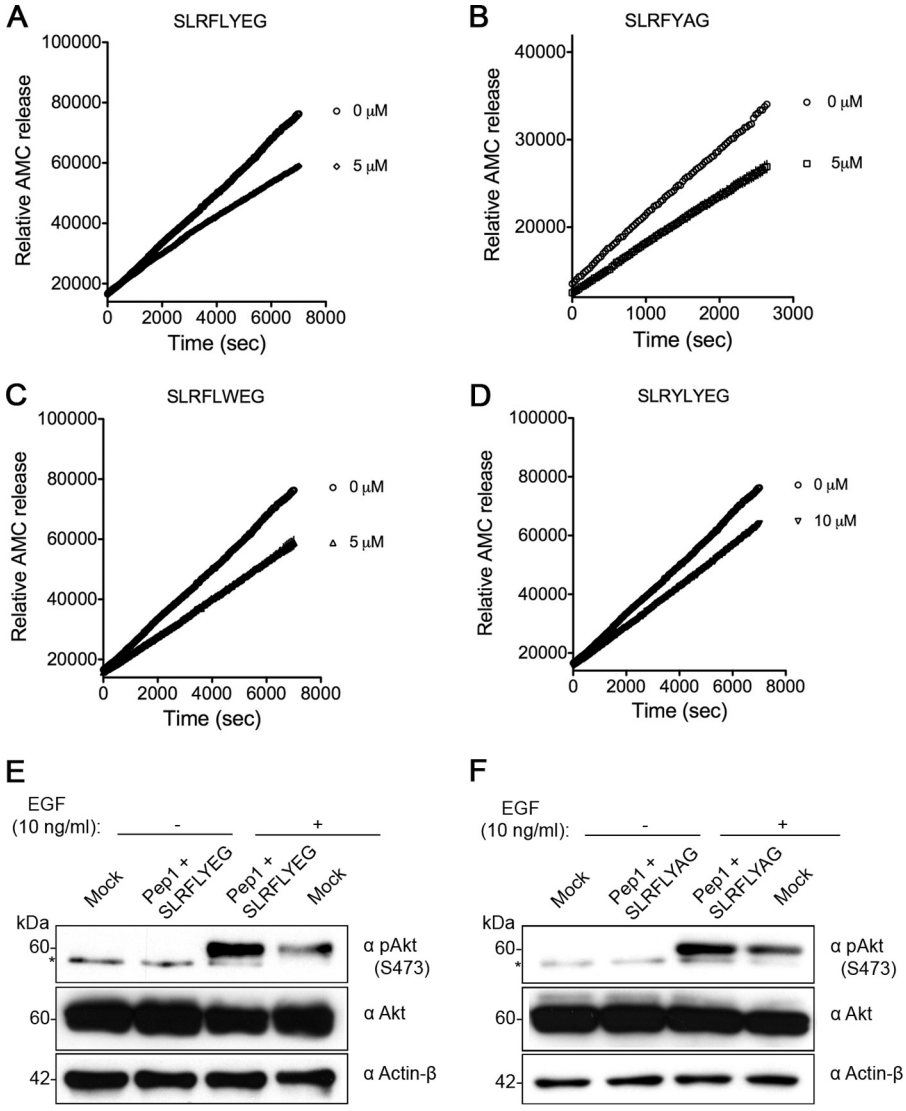

FIGURE 6. **Inhibition of endogenous DPP8 and DPP9 by SLRFLYEG and its variants in intact cells.** *A–D*, inhibitory EIL peptide variant. SLR*XLXX*G was complexed with the carrier peptide (Pep-1). HeLa cells were incubated for 30 min at 37 °C with a complex containing the SLR*XLXX*G inhibitory peptide and the Pep-1 carrier peptide. Cytosolic extracts were then tested for hydrolysis of GP-AMC over time. All experiments described were performed at least three independent times. *A*, 5 μM SLRFL**Y**EG was complexed with the carrier peptide Pep-1. For control, HeLa cells were incubated with Pep-1 only. *B*, same as in *A* but with SLRFL**YA**G. *C*, same as in *A* but with SLRFL**W**EG. *D*, same as in *A* but with but with 10 μM SLR**Y**L**Y**EG. *E*, HeLa cells were incubated for 25 min with the Pep-1-SLRFLYEG complex at 37 °C, followed by a 5-min induction with EGF (10 ng/ml). Samples were immediately lysed in sample buffer and analyzed by Western blotting with specific antibodies. *F*, same as in *E*, but with the SLRFLYAG peptide.

EIL-SUMO1 peptide. However, whereas DPP9V285A completely loses interaction with the full-length SUMO1 protein, it does not completely lose its sensitivity to the SUMO1-EIL peptide, as measured by a 2-fold increase in K_i value, suggesting a 50% drop in affinity. This difference implies that the interaction of the isolated EIL peptide with DPP9 is not identical to the interaction of full-length SUMO1 with DPP9 and may result from a slightly altered conformation of the EIL as an isolated peptide compared with its structure in the folded SUMO1 protein. For example, solved structures of SUMO1 show that serine 61, leucine 62, and phenylalanine 64 of SUMO1 are buried in the full-length protein. However, they may be exposed in the EIL peptide and thus affect the interaction with DPP9. In contrast to DPP9V285A mutant, which is impaired in activity, the DPP9 variant mutated at Tyr-303 is only slightly impaired in enzymatic activity, as measured by K_{cat} and K_m values. Nonetheless, the DPP9Y303 mutant also loses its sensitivity to the EIL peptide, showing a 2-fold increase in K_i compared with the wild-type enzyme, thus unlinking intrinsic enzymatic activity from interaction with the peptide. In summary, inhibition of DPP9 by the EIL peptide and its variants is dependent on single residues in the DPP9 arm. Taken together, these results suggest that the EIL and its variants act as novel allosteric inhibitors of DPP9. Crystal structures of DPP9 in complex with the EIL or SLRFLYEG will provide more details regarding the exact residues that participate in this interaction and a better understanding of the mechanism leading to DPP9 inhibition by these peptides.

The analysis of the activity of multiple point mutation in the DPP9 arm stresses the role of the arm for enzymatic activity. Single and double point mutations in the DPP9 arm, such as Glu-278, Glu-279, Asp-281, Glu-282, and Tyr-305, lead to a

strong impairment in peptidase activity. A DPP9 homology model (26) predicts that these amino acids are located to the inner edge of the arm, on the hinge connecting the arm to the propeller. The predicted localization to the hinge suggests that the reduced enzymatic activity may result from a change in the molecular localization of the arm and may imitate a natural dynamic or movement in this region. Thus, the arm of DPP9 is an important motif for enzymatic activity and for allosteric regulation of the peptidase.

All inhibitors described so far are competitive and target both DPP8 and DPP9 (32–36). The best selectivity was described recently by Van Goethem *et al.* (36), who systematically dissected and modified the DPP8/9 inhibitor 1G244 to increase the selectivity of the inhibitor toward DPP8. This analysis led to identification of compound 12n, which showed a 10-fold selectivity toward DPP8 when measuring IC_{50} values and a 6.4 selectivity for DPP8 over DPP9 in K_i values (36). Allosteric inhibitors are emerging as a promising alternative approach to competitive inhibitors, which are more prone to off-target side effects caused by the high conservation of the catalytic sites (37–39). Amino acid alignment analysis of DPP8, DPP9, and DPPIV shows a lower conservation of the arm compared with the active site of the DPP enzymes. DPP8 and DPP9 share 72% similarity in the arm, compared with catalytic pockets, which is 90% identical. Here we observed that an exchange of single amino acids in the EIL peptide variants can give a preference for inhibition of DPP8 over DPP9. For example, SLRFLWEG possesses 4.5-fold selectivity for DPP8 over DPP9, as measured in K_i values. We propose that further modifications of the allosteric peptide inhibitors described here, such as SLRFLWEG, are promising leads for the development of inhibitors with higher selectivity toward DPP8 or DPP9, to circumvent the problem posed by the high conservation in the catalytic domain of DPP8 and DPP9 (27, 36). Furthermore, the conservation of the arm motif is even lower for DPPIV, which shares only ~28% similarity with DPP8 and DPP9 in the arm motif. In line with this, SLRFLYEG possesses more than 1,000-fold selectivity for DPP8 and DPP9 over DPPIV. For comparison, vildagliptin, which is an approved drug for treatment of diabetes type II, displays only a 32-fold selectivity toward DPPIV over DPP9, with $K_i$values of 3 and 95 nM, respectively (40).

Importantly, here we show that the SLR*XLXXG* peptide variants can be used to inhibit DPP8 and DPP9 in intact cells, in combination with Pep-1 (Ref. 29; reviewed in Refs. 30 and 31). Using this method, application of SLRFLYEG, SLRFLWEG, and SLRFLYAG leads to a significant and comparable reduction of ~30% in cytosolic prolyl-peptidase activity. Apart from the SLR*XLXXG* peptides described here, the only DPP8/9 inhibitor that was clearly shown to penetrate the cell membrane is 1G244 (35). In this case, the addition of 1.6 or 8 μM of 1G244 to cells for 6 h resulted in a 40 and 60% reduction in cellular DPP activity, respectively (35). For comparison, in combination with Pep-1, the application of 5 μM SLRFLYEG or SLRFLYAG results in a 30% reduction of cellular DPP activity, already after 30 min of incubation.

Furthermore, treatment of HeLa cells with SLRFLYAG or SLRFLYEG leads to an increase in EGF-mediated phosphorylation of Akt, compared with untreated cells. This effect confirms previous results obtained with a DPP8/9 inhibitor that targets the active site of these enzymes (22). However, in the experiments described here, the cells did not overexpress DPP9, showing that inhibition of endogenous DPP9 with these novel allosteric inhibitors is sufficient for modulating the Akt pathway. Therefore our results not only demonstrate the applicability of SLRFLYEG and SLRFLYAG for studying the regulation and activity of recombinant DPP8 and DPP9 but are also applicable for studies of these endogenous peptidases within cells. In summary, this work highlights the potential use of peptides that mimic interaction surfaces as tools for modulating and studying enzyme activity.

Acknowledgments—We are very are grateful to Blanche Schwappach and Daniela Justa-Schuch for critical reading of the manuscript, members of the Geiss-Friedlander group for stimulating discussions, and Blanche Schwappach for very generous support.

REFERENCES

1. Rawlings, N. D., Barrett, A. J., and Bateman, A. (2010) MEROPS. The peptidase database. *Nucleic Acids Res.* **38,** D227–D233
2. Vanhoof, G., Goossens, F., De Meester, I., Hendriks, D., and Scharpé, S. (1995) Proline motifs in peptides and their biological processing. *FASEB J.* **9,** 736–744
3. Rosenblum, J. S., and Kozarich, J. W. (2003) Prolyl peptidases. A serine protease subfamily with high potential for drug discovery. *Curr. Opin. Chem. Biol.* **7,** 496–504
4. Yu, D. M., Yao, T.-W., Chowdhury, S., Nadvi, N. A., Osborne, B., Church, W. B., McCaughan, G. W., and Gorrell, M. D. (2010) The dipeptidyl peptidase IV family in cancer and cell biology. *FEBS J.* **277,** 1126–1144
5. Zhang, H., Chen, Y., Keane, F. M., and Gorrell, M. D. (2013) Advances in understanding the expression and function of dipeptidyl peptidase 8 and 9. *Mol. Cancer Res.*, 10.1158/1541-7786.MCR-13-0272
6. Wolf, B. B., Quan, C., Tran, T., Wiesmann, C., and Sutherlin, D. (2008) On the edge of validation. Cancer protease fibroblast activation protein. *Mini. Rev. Med. Chem.* **8,** 719–727
7. Kim, D., Wang, L., Beconi, M., Eiermann, G. J., Fisher, M. H., He, H., Hickey, G. J., Kowalchick, J. E., Leiting, B., Lyons, K., Marsilio, F., McCann, M. E., Patel, R. A., Petrov, A., Scapin, G., Patel, S. B., Roy, R. S., Wu, J. K., Wyvratt, M. J., Zhang, B. B., Zhu, L., Thornberry, N. A., and Weber, A. E. (2005) (2*R*)-4-Oxo-4-[3-(trifluoromethyl)-5,6-dihydro[1,2,4]triazolo[4,3-a]pyrazin-7(8H)-yl]-1-(2,4,5-trifluorophenyl)butan-2-amine. A potent, orally active dipeptidyl peptidase IV inhibitor for the treatment of type 2 diabetes. *J. Med. Chem.* **48,** 141–151
8. Augeri, D. J., Robl, J. A., Betebenner, D. A., Magnin, D. R., Khanna, A., Robertson, J. G., Wang, A., Simpkins, L. M., Taunk, P., Huang, Q., Han, S.-P., Abboa-Offei, B., Cap, M., Xin, L., Tao, L., Tozzo, E., Welzel, G. E., Egan, D. M., Marcinkeviciene, J., Chang, S. Y., Biller, S. A., Kirby, M. S., Parker, R. A., and Hamann, L. G. (2005) Discovery and preclinical profile of saxagliptin (BMS-477118). A highly potent, long-acting, orally active dipeptidyl peptidase IV inhibitor for the treatment of type 2 diabetes. *J. Med. Chem.* **48,** 5025–5037
9. Villhauer, E. B., Brinkman, J. A., Naderi, G. B., Burkey, B. F., Dunning, B. E., Prasad, K., Mangold, B. L., Russell, M. E., and Hughes, T. E. (2003) 1-[[(3-Hydroxy-1-adamantyl)amino]acetyl]-2-cyano-(*S*)-pyrrolidine. A potent, selective, and orally bioavailable dipeptidyl peptidase IV inhibitor with antihyperglycemic properties. *J. Med. Chem.* **46,** 2774–2789
10. McIntosh, C. H., Demuth, H.-U., Pospisilik, J. A., and Pederson, R. (2005) Dipeptidyl peptidase IV inhibitors. How do they work as new antidiabetic agents? *Regul. Pept.* **128,** 159–165
11. Spagnuolo, P. A., Hurren, R., Gronda, M., MacLean, N., Datti, A., Basheer, A., Lin, F.-H., Wang, X., Wrana, J., and Schimmer, A. D. (2013) Inhibition of intracellular dipeptidyl peptidases 8 and 9 enhances parthenolide's anti-leukemic activity. *Leukemia* **27,** 1236–1244

12. Abbott, C. A., Yu, D. M., Woollatt, E., Sutherland, G. R., McCaughan, G. W., and Gorrell, M. D. (2000) Cloning, expression and chromosomal localization of a novel human dipeptidyl peptidase (DPP) IV homolog, DPP8. *Eur. J. Biochem.* **267,** 6140–6150
13. Olsen, C., and Wagtmann, N. (2002) Identification and characterization of human DPP9, a novel homologue of dipeptidyl peptidase IV. *Gene* **299,** 185–193
14. Ajami, K., Abbott, C. A., McCaughan, G. W., and Gorrell, M. D. (2004) Dipeptidyl peptidase 9 has two forms, a broad tissue distribution, cytoplasmic localization and DPIV-like peptidase activity. *Biochim. Biophys. Acta* **1679,** 18–28
15. Geiss-Friedlander, R., Parmentier, N., Möller, U., Urlaub, H., Van den Eynde, B. J., and Melchior, F. (2009) The cytoplasmic peptidase DPP9 is rate-limiting for degradation of proline-containing peptides. *J. Biol. Chem.* **284,** 27211–27219
16. Vigneron, N., and Van den Eynde, B. J. (2011) Insights into the processing of MHC class I ligands gained from the study of human tumor epitopes. *Cell. Mol. Life Sci.* **68,** 1503–1520
17. van Endert, P. (2011) Post-proteasomal and proteasome-independent generation of MHC class I ligands. *Cell. Mol. Life Sci.* **68,** 1553–1567
18. Wilson, C. H., Indarto, D., Doucet, A., Pogson, L. D., Pitman, M. R., McNicholas, K., Menz, R. I., Overall, C. M., and Abbott, C. A. (2013) Identifying natural substrates for dipeptidyl peptidase 8 (DP8) and DP9 using terminal amine isotopic labelling of substrates, TAILS, reveals in vivo roles in cellular homeostasis and energy metabolism. *J. Biol. Chem.* **288,** 13936–13949
19. Lu, C., Tilan, J. U., Everhart, L., Czarnecka, M., Soldin, S. J., Mendu, D. R., Jeha, D., Hanafy, J., Lee, C. K., Sun, J., Izycka-Swieszewska, E., Toretsky, J. A., and Kitlinska, J. (2011) Dipeptidyl peptidases as survival factors in Ewing sarcoma family of tumors. Implications for tumor biology and therapy. *J. Biol. Chem.* **286,** 27494–27505
20. Matheeussen, V., Waumans, Y., Martinet, W., Van Goethem, S., Van der Veken, P., Scharpé, S., Augustyns, K., De Meyer, G. R., and De Meester, I. (2013) Dipeptidyl peptidases in atherosclerosis. Expression and role in macrophage differentiation, activation and apoptosis. *Basic Res. Cardiol.* **108,** 350
21. Yu, D. M., Wang, X. M., McCaughan, G. W., and Gorrell, M. D. (2006) Extraenzymatic functions of the dipeptidyl peptidase IV-related proteins DP8 and DP9 in cell adhesion, migration and apoptosis. *FEBS J.* **273,** 2447–2460
22. Yao, T.-W., Kim, W.-S., Yu, D. M., Sharbeen, G., McCaughan, G. W., Choi, K.-Y., Xia, P., and Gorrell, M. D. (2011) A novel role of dipeptidyl peptidase 9 in epidermal growth factor signaling. *Mol. Cancer Res.* **9,** 948–959
23. Schade, J., Stephan, M., Schmiedl, A., Wagner, L., Niestroj, A. J., Demuth, H.-U., Frerker, N., Klemann, C., Raber, K. A., Pabst, R., and von Hörsten, S. (2008) Regulation of expression and function of dipeptidyl peptidase 4 (DP4), DP8/9, and DP10 in allergic responses of the lung in rats. *J. Histochem. Cytochem.* **56,** 147–155
24. Sulda, M. L., Abbott, C. A., Macardle, P. J., Hall, R. K., and Kuss, B. J. (2010) Expression and prognostic assessment of dipeptidyl peptidase IV and related enzymes in B-cell chronic lymphocytic leukemia. *Cancer Biol. Ther.* **10,** 180–189
25. Pilla, E., Möller, U., Sauer, G., Mattiroli, F., Melchior, F., and Geiss-Friedlander, R. (2012) A novel SUMO1-specific interacting motif in dipeptidyl peptidase 9 (DPP9) that is important for enzymatic regulation. *J. Biol. Chem.* **287,** 44320–44329
26. Park, J., Knott, H. M., Nadvi, N. A., Collyer, C. A., Wang, X. M., Church, W. B., and Gorrell, M. D. (2008) Reversible inactivation of human dipeptidyl peptidases 8 and 9 by oxidation. *TOEIJ* **1,** 52–60
27. Rummey, C., and Metz, G. (2007) Homology models of dipeptidyl peptidases 8 and 9 with a focus on loop predictions near the active site. *Proteins* **66,** 160–171
28. Tang, H.-K., Chen, K.-C., Liou, G.-G., Cheng, S.-C., Chien, C.-H., Tang, H.-Y., Huang, L.-H., Chang, H.-P., Chou, C.-Y., and Chen, X. (2011) Role of a propeller loop in the quaternary structure and enzymatic activity of prolyl dipeptidases DPP-IV and DPP9. *FEBS Lett.* **585,** 3409–3414
29. Morris, M. C., Depollier, J., Mery, J., Heitz, F., and Divita, G. (2001) A peptide carrier for the delivery of biologically active proteins into mammalian cells. *Nat. Biotechnol.* **19,** 1173–1176
30. Deshayes, S., Morris, M. C., Divita, G., and Heitz, F. (2005) Cell-penetrating peptides. Tools for intracellular delivery of therapeutics. *Cell. Mol. Life Sci.* **62,** 1839–1849
31. Morris, M. C., Deshayes, S., Heitz, F., and Divita, G. (2008) Cell-penetrating peptides. From molecular mechanisms to therapeutics. *Biol. Cell* **100,** 201–217
32. Jiaang, W.-T., Chen, Y.-S., Hsu, T., Wu, S.-H., Chien, C.-H., Chang, C.-N., Chang, S.-P., Lee, S.-J., and Chen, X. (2005) Novel isoindoline compounds for potent and selective inhibition of prolyl dipeptidase DPP8. *Bioorg. Med. Chem. Lett.* **15,** 687–691
33. Van der Veken, P., Soroka, A., Brandt, I., Chen, Y.-S., Maes, M.-B., Lambeir, A.-M., Chen, X., Haemers, A., Scharpé, S., Augustyns, K., and De Meester, I. (2007) Irreversible inhibition of dipeptidyl peptidase 8 by dipeptide-derived diaryl phosphonates. *J. Med. Chem.* **50,** 5568–5570
34. Lankas, G. R., Leiting, B., Roy, R. S., Eiermann, G. J., Beconi, M. G., Biftu, T., Chan, C.-C., Edmondson, S., Feeney, W. P., He, H., Ippolito, D. E., Kim, D., Lyons, K. A., Ok, H. O., Patel, R. A., Petrov, A. N., Pryor, K. A., Qian, X., Reigle, L., Woods, A., Wu, J. K., Zaller, D., Zhang, X., Zhu, L., Weber, A. E., and Thornberry, N. A. (2005) Dipeptidyl peptidase IV inhibition for the treatment of type 2 diabetes. Potential importance of selectivity over dipeptidyl peptidases 8 and 9. *Diabetes* **54,** 2988–2994
35. Wu, J.-J., Tang, H.-K., Yeh, T.-K., Chen, C.-M., Shy, H.-S., Chu, Y.-R., Chien, C.-H., Tsai, T.-Y., Huang, Y.-C., Huang, Y.-L., Huang, C.-H., Tseng, H.-Y., Jiaang, W.-T., Chao, Y.-S., and Chen, X. (2009) Biochemistry, pharmacokinetics, and toxicology of a potent and selective DPP8/9 inhibitor. *Biochem. Pharmacol.* **78,** 203–210
36. Van Goethem, S., Matheeussen, V., Joossens, J., Lambeir, A.-M., Chen, X., De Meester, I., Haemers, A., Augustyns, K., and Van der Veken, P. (2011) Structure-activity relationship studies on isoindoline inhibitors of dipeptidyl peptidases 8 and 9 (DPP8, DPP9). Is DPP8-selectivity an attainable goal? *J. Med. Chem.* **54,** 5737–5746
37. Hauske, P., Ottmann, C., Meltzer, M., Ehrmann, M., and Kaiser, M. (2008) Allosteric regulation of proteases. *Chembiochem* **9,** 2920–2928
38. Tsai, C.-J., del Sol, A., and Nussinov, R. (2008) Allostery. Absence of a change in shape does not imply that allostery is not at play. *J. Mol. Biol.* **378,** 1–11
39. Merdanovic, M., Mönig, T., Ehrmann, M., and Kaiser, M. (2013) Diversity of allosteric regulation in proteases. *ACS Chem. Biol.* **8,** 19–26
40. Burkey, B. F., Hoffmann, P. K., Hassiepen, U., Trappe, J., Juedes, M., and Foley, J. E. (2008) Adverse effects of dipeptidyl peptidases 8 and 9 inhibition in rodents revisited. *Diabetes Obes. Metab.* **10,** 1057–1061